Nanoscale

PAPER

View Article Online
View Journal | View Issue

Cite this: *Nanoscale*, 2016, **8**, 16405

The dissipation of field emitting carbon nanotubes in an oxygen environment as revealed by *in situ* transmission electron microscopy†

Ai Leen Koh,*[a] Emily Gidcumb,[b] Otto Zhou[b,c] and Robert Sinclair*[d]

In this work, we report the first direct experimental observations of carbon nanotubes (CNT) field emitting in an oxygen environment, using aberration-corrected environmental transmission electron microscopy in combination with an electrical biasing specimen holder under low-dose, field-free imaging conditions. Our studies show that while the CNTs remain stable during high vacuum field emission, they experience abrupt decreases in length, also termed "burn-back", when field-emitting in an oxygen environment at around 30 Pa pressure. Furthermore, we perform correlative field-free and aberration-corrected, high-resolution transmission electron microscopy imaging to understand how the structure of the CNTs – particularly the opening of the nanotube caps – is influenced by its gas environment during field emission. This work provides significant insight into the mechanism of carbon nanotube behavior under non-ideal field emission conditions.

Received 5th August 2016,
Accepted 22nd August 2016

DOI: 10.1039/c6nr06231h

www.rsc.org/nanoscale

Introduction

One of the major technological applications of carbon nanotubes (CNT)[1] is as field emission electron sources to generate high intensity X-rays for medical devices.[2–5] For optimum performance, CNT-based electron sources are housed in vacuum chambers with base pressures of 10^{-5} Pa or better.[6,7] Under less stringent vacuum conditions, CNTs are found to exhibit reduced emission currents and shorter lifetimes.[6,8] Dean and co-workers reported that the emission currents of single-walled CNTs decreased when they were emitting in low pressures of oxygen, and hypothesized that this was probably due to reactive sputter etching leading to the decrease in nanotube heights, destruction of small diameter tubes through ion bombardment, the opening of the nanotube cap, or the disruption of electronic states in the cap.[8]

On the other hand, the oxidation of CNTs has both technological and scientific importance. For instance, some authors have used oxidation to refine the nanotube lengths[9] or enhance the chemical reactivity of their graphitic network[10] for various applications.[11] For use as field emission electron sources, it was thought that the opening of nanotube caps under mild oxidizing conditions can result in a hundred-fold increase in current.[12] In contrast to what had been reported by Dean *et al.*,[8] Zhang and coworkers[13] observed that the addition of oxygen gas to CNT pixel arrays during field emission does *not* reduce emission stability. The same group examined different CNTs nanotubes before and after oxygen treatment and concluded that nanotubes roughen with oxygen treatment and some are removed by excessive field emission.[13] However, given the heterogeneous nature of the samples, it is difficult to draw a conclusion about individual CNTs from the work.

Shortly after the discovery of CNTs, several research groups attempted to utilize the oxidation process to manipulate their structures. They had proposed, by *post facto* observations, that the nanotubes oxidize first at their curved tips, followed by layer-by-layer removal of the outermost graphene sheets.[14,15] However, our recent *quasi in situ* studies in an environmental transmission electron microscope (ETEM), with the electron beam blanked during oxidation in the temperature range 300–520 °C, suggest that the nanotube tips are stable and that the molecular oxidation mechanism occurs primarily by the layer-by-layer attack starting from the outermost tube wall.[16]

[a]*Stanford Nano Shared Facilities, Stanford University, Stanford, California 94305, USA. E-mail: alkoh@stanford.edu*
[b]*Department of Applied Physical Sciences, University of North Carolina at Chapel Hill, Chapel Hill, North Carolina 27599, USA*
[c]*Department of Physics and Astronomy, University of North Carolina at Chapel Hill, Chapel Hill, North Carolina 27599, USA*
[d]*Department of Materials Science and Engineering, Stanford University, Stanford, California 94305, USA. E-mail: bobsinc@stanford.edu*

†Electronic supplementary information (ESI) available: Stable field emission of CNTs in high vacuum over time. Alignment of CNTs with applied bias. Individual, consecutive, frames extracted from an *in situ* dataset recorded using the OneView camera at 25 fps (40 ms time resolution) during field emission in 34 Pa oxygen pressure and −100 V applied bias. (pdf). Video clip of CNTs field emission in 34 Pa of oxygen (avi). See DOI: 10.1039/c6nr06231h

The situation with the imaging electron beam illuminating the sample is quite different. With the electron beam un-blanked, the removal of the material from the nanotubes was observed both at their tips and along the periphery, even at room temperature, due to the ionization of the oxygen gas by the electron beam during the recordings.[17] This reaction is induced by the electron beam, as graphite and oxygen are known to not react with each other at this temperature.

The two approaches, namely blanking and un-blanking of the electron beam in the presence of gas, enable us to understand how the electron beam can influence outcomes in *in situ* ETEM experiments. We also realize that during the field emission process in an oxygen environment, the field emitting nanotubes are also likely to ionize the oxygen molecules locally. To be able to identify the oxidation process of field emitting nanotubes unambiguously, it is clearly necessary to observe the reaction *in situ*, under field-emitting conditions, and at the same time to eliminate the influence of the electron beam. We show that this is possible by combining an electrical biasing holder with the ETEM oxygen environment and using low electron beam irradiation conditions to avoid the beam influencing the behavior.

In this work, we report for the first time direct experimental observations of carbon nanotubes (CNTs) field emitting in a controlled oxygen environment, using aberration-corrected environmental transmission electron microscopy (ETEM) in combination with an electrical biasing specimen holder under low-dose, field-free imaging conditions. The combination of electrical biasing with the gas environment significantly compounds the difficulty of successful observations in the TEM. Under an applied electric field, free-standing carbon nanotubes 'vibrate' and this instability leads to difficulties in imaging them at the high resolution and magnification of a TEM. Specimen drift is also more likely to occur in a gas environment compared to high vacuum conditions. Furthermore, the electron beam can also ionize molecular gas species and influence the experimental outcome. Therefore, careful experimental design which precludes the influence of the electron beam needs to be made, as we will discuss in this article. Our studies show that while the CNTs can remain stable during high vacuum field emission, they experience abrupt decreases in length when field-emitting in an oxygen environment. Furthermore, aberration-corrected, high-resolution transmission electron microscopy (ACTEM) data reveal how the structure of the CNTs is influenced by its gas environment during field emission, particularly the opening of the nanotube caps. This work provides significant insight into the mechanism of carbon nanotube behavior under field emission conditions in oxygen gas.

Experimental

Sample preparation

Multiwalled carbon nanotubes (CNTs) synthesized by the arc discharge method[18] were used in this study. They were first sonicated in ethyl alcohol, and the suspension was drop cast onto Cu TEM grids with ultrathin C support film (Ted Pella Inc.) which had been cut in half, and then wicked dry using filter paper. The half-TEM grid was then attached to a Cu wire using conductive epoxy (Circuit Works), and mounted onto one end of an electrical biasing holder (Nanofactory Inc.).

TEM experiments

An electrical biasing holder (Nanofactory Inc.) was used for all the experiments reported in this paper. The holder consists of a piezoelectrically-controlled tube with a rigid sapphire ball and a "tipholder" onto which a Pt/Ir scanning tunneling microscope (STM) probe (DPT10, Bruker Inc.) is attached.[19] At the start of the experiment, the half-TEM grid containing the carbon nanotubes was first adjusted to eucentric height. Then, the piezoelectric controls of the Nanofactory holder were used to independently adjust the STM tip to the same height as that of the carbon nanotubes. Since carbon nanotube samples are in bundles, the height of individual tubes within the bundle could vary. Typically, one (or a few) carbon nanotubes within the bundle would be identified for field emission at the start of the experiment, and the height of the STM tip would be adjusted to that of the intended nanotube (s). We know that the identified nanotubes and tip are at the same height when both are in focus at the same time (minimum TEM image contrast).

Experiments were performed at room temperature using a FEI Titan 80–300 kV environmental TEM operated at 80 kV, which is below the knock-on displacement energy of carbon atoms in single wall carbon nanotubes.[20] The instrument is equipped with a spherical aberration (Cs) corrector in the objective lens and a Lorentz lens. The instrument resolution is ~0.1 nm with the objective lens on, and ~2 nm in the Lorentz mode at 80 kV. TEM images were acquired using an Ultrascan 1000XP CCD camera (Gatan Inc.) and a OneView CMOS-based camera (Gatan Inc.). The data presented in Fig. 2b was part of a continuous recording using the US1000XP at 20 fps frame speed (50 ms per frame) using CamStudio software. Frames were extracted using VirtualDub, and analyzed using ImageJ.

For ETEM experiments, oxygen of Grade 6.0 (99.9999%, AirLiquide Inc.) purity, and pressure not exceeding 70 Pa (0.7 mbar), was used in all our experiments. The actual pressure in the ETEM chamber was monitored using an Edwards Barocell 600 capacitance manometer with which the microscope is equipped.

All field emission experiments were performed in Lorentz mode, whereby the highly magnetizing objective lens is turned off and the specimen experiences no magnetic field. Fortuitously, this operating mode also provides a low beam dosage rate (by a factor of approximately 20 compared to that with the objective lens on), as the imaging magnification is necessarily much lower, and the imaging beam more spread, than when imaging using the objective lens. Thus, the imaging conditions are below the threshold for CNT degradation under vacuum or oxygen environment.[17]

Aberration-corrected, high resolution TEM imaging and dose conditions

All aberration-corrected, high-resolution TEM images were acquired under high vacuum conditions (microscope base pressure of 10^{-5} to 10^{-6} Pa), with the Cs value adjusted close to 0 μm, and at slightly underfocus conditions. The average electron dose flux was 1×10^3 e^- $Å^{-2}$ s^{-1} (1×10^5 e^- nm^{-2} s^{-1}), and the average time per frame was 0.3 seconds.

Image rotation

There is an image rotation of 90 degrees between the high-resolution (objective lens on) and Lorentz (objective lens off) modes of the TEM. In our figures, all high-resolution images have been rotated by 90 degrees with respect to the field-free images.

Results and discussion

Sample preparation and experimental setup

Fig. 1a shows a photograph of the electrical biasing holder used in this work. The half-TEM grid with CNTs is on the right (III). The other end consists of a piezoelectrically-controlled tube with a rigid sapphire ball (I) and a "tipholder" onto which the Pt/Ir STM probe is attached (II).[19] Fig. 1b shows a low-magnification TEM image of the setup acquired in Lorentz mode. Only nanotubes that extend from the edge of the half-grid can come into close proximity with the STM tip and can thus be field-emitted. The CNTs in this study are the same raw materials that would be used towards fabrication of high intensity X ray sources. We opted to study the nanotubes as synthesized, which are in the form of bundles surrounded by an amorphous carbon overcoat, without further sample treatment. Although they appear in bundles, the concentration of the nanotubes was low enough for us to discern individual ones and perform correlative Lorentz and ACTEM analysis on each tube (see later sections). The nanotubes appeared to adhere well to the half-TEM grid for all the voltage bias and compliance settings that we had used in our study. Accordingly, we did not find it necessary to employ additional nanotube-to-substrate adhesion mechanisms for this work.

The nanotubes were positioned approximately 500 nm to 1 μm away from the tip using the piezoelectric control. This distance refers to that between the STM tip and nanotube that was co-located at the same height at the start of the experiment. Fig. 1c and d are higher-magnification TEM images

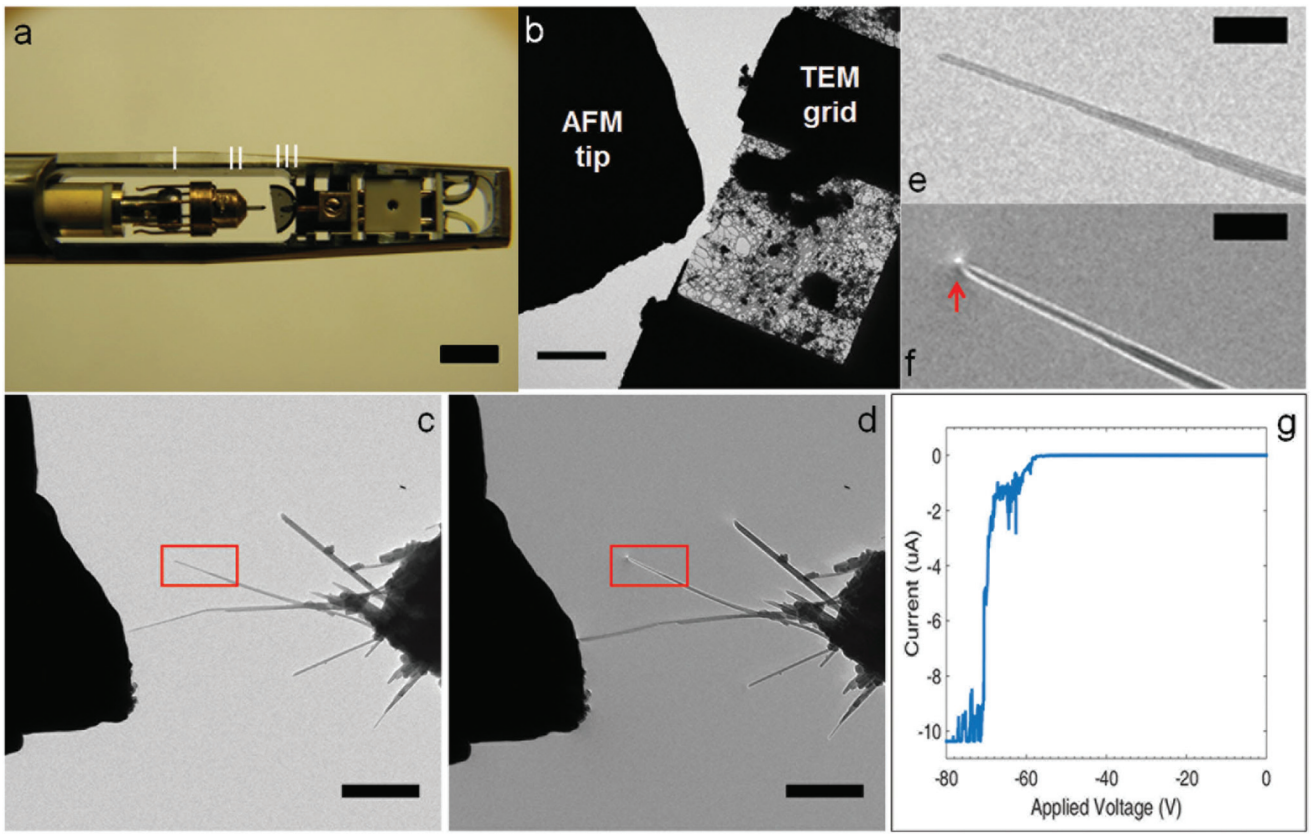

Fig. 1 (a) Photograph of electrical biasing holder used in this study. (b) Low-magnification Lorentz TEM image acquired at 80 kV showing STM tip and TEM grid. (c) and (d) are higher magnification Lorentz TEM images acquired at 80 kV, showing the end of a STM tip on the left of the image, and a bundle of multiwalled CNTs at the right of the image, acquired under applied voltages of 0 V and −80 V, respectively. (e) and (f) show higher-magnification images of the insets indicated by red boxes in (c) and (d). (g) Representative *I*–*V* curve showing high vacuum field emission characteristics of carbon nanotubes investigated in this study. Scale markers equal 5 mm in (a), 25 μm in (b), 1 μm in (c) and (d), and 200 nm in (e) and (f).

acquired in field-free mode showing the end of an STM tip on the left of the image, and a bundle of CNTs on the right of the image, under holder voltage biases of 0 V and −80 V, respectively. With an applied bias, a bright contrast at the tip, which is caused by electric fields around the nanotube associated with field emission, can be observed (Fig. 1d).[21] The electric field strength is highest at the nanotube tips (Fig. 1e and f), which has been confirmed using electron holography.[22–24] Field emission was demonstrated by current–voltage (*I–V*) curve measurements recorded concurrently with the TEM experiments, a representative example of which is presented in Fig. 1g. These values are in a similar range to those reported previously.[22,25,26] The *I–V* curve presented in Fig. 1g shows abrupt fluctuations at low voltage, which can be due to the presence of adsorbates on the nanotube surface which enhance the field emission current, as reported previously.[26,27]

In situ high vacuum field emission

First, control experiments were performed to study the CNT behavior under high vacuum (10^{-5} Pa) field emission. We set up the field emission experiment such that the CNTs would emit in a stable manner over a long period of time (*i.e.* at a relatively mild applied voltage and field emission current), as previous studies have shown.[6,8] We avoided working at excessive field emission voltages and currents, which had been known to cause structural modifications and damage to CNTs even in high vacuum.[6,28–32] This was confirmed by our direct observations in the microscope, accompanied by the measured field emission current. High vacuum field emission experiments were performed on ~40 CNTs using compliance current settings of 1 μA and 10 μA. The CNTs exhibited similar behavior under these two compliance current settings. They would field emit in a stable manner in high vacuum for relatively long periods of time (10–15 min) without any apparent change in structure (Fig. 2a) or emission current (ESI Fig. 1†). In addition, the initially randomly oriented CNTs were observed to align parallel to the electric field upon the application of a bias, and returned approximately to their original orientation when the bias was turned off (ESI Fig. 2†), a phenomenon which had been reported previously.[30,33]

Oxygen environment field emission

Having established the stability of the CNTs under high vacuum field emission, 24 Pa of oxygen (99.9999% purity) was introduced into the ETEM, and the measurements were repeated on the same set of nanotubes presented in Fig. 2a after sample stability had been restored (~1 hour). Fig. 2b(i–viii) are TEM images extracted from a video clip recorded at 20 frames per second (fps) (0.05 s per frame) (see ESI Video S1†). When the applied voltage was increased from −50 V to −70 V (Fig. 2b(ii)–(iii)), there was a sudden reduction in length of approximately 400 nm in one of the CNTs (red arrow) within 50 ms. This nanotube was initially at a different height from the STM tip and was not field-emitting in high vacuum, as observed by the absence of the bright intensity at its tip. However, its relative height could have changed at the end of the high vacuum field emission to be co-located with that of the tip. This in turn enabled its field emission in oxygen (Fig. 2b). One second later, the same nanotube continued to experience a further, abrupt reduction in its length (Fig. 2b(iv)) while the applied voltage bias was maintained at −70 V. At −80 V (Fig. 2b(v)), another nanotube (indicated by blue triangles) was abruptly shortened (410 nm in 50 ms, Fig. 2b(vi)). In the same frame sequence, the nanotube with the red arrow experienced another length reduction of approximately 90 nm. In addition, multiple field emission spots at the tips, indicated by the presence of two, bright intensity spots (yellow stars in Fig. 2b(vii)), were observed. This was attributed to multiple nanotubes in one bundle, as we will discuss later. The nanotube bundle shows significant length reductions after field emitting in oxygen for 519 seconds (Fig. 2b(i) and (viii)). Examinations of the recordings show that such events occur between individual frames (down to 40 ms time resolution, ESI Fig. 3†), suggesting that a large number of carbon atoms were removed simultaneously. These reductions amount to $\sim 2.5 \times 10^6$ (90 nm length reduction) to 1.1×10^7 (410 nm) carbon atoms, as estimated from the CNT widths and lengths involved.[16] The nanotube then remains, still field-emitting, until another such event occurs after several more seconds. Clearly this is not occurring in a layer-by-layer mechanism as in the molecular oxidation non-biasing situation. Eventually the whole nanotube is consumed and is no longer available for field emission, consistent with the decrease of total field emission current under oxidation conditions.[8]

ESI Fig. 3† shows individual frames extracted from an *in situ* dataset recorded using a 4096-by-4096 pixel OneView CMOS based camera (Gatan Inc.) with a recording speed of 25 fps (40 ms per frame) during field emission in 34 Pa oxygen and −100 V applied bias. Each frame was a 4096-by-4096 pixel image. Consecutive frames revealing abrupt changes in CNT lengths were identified, and subtracted, to measure the changes in CNT length. Oxygen field emission experiments were performed on ~40 CNTs (different from those studied under high vacuum field emission in this case) using compliance current settings of 1 μA and 10 μA. The behavior of abrupt decreases in nanotube lengths was consistent in both settings.

Fig. 3 shows the field emission current characteristics for the *in situ* oxygen field emission data which had been presented in Fig. 2(b) and in ESI Video S1.† The top of the horizontal axis shows the corresponding applied bias in the time series. By correlating the video to the field emission current plot, we observed that when the applied bias was increased from −50 V to −70 V at around 86 s (or 1.41 min), there was a brief increase in emission current. Soon after, there was an abrupt shortening of the nanotube, which corresponded to a reduction in the recorded emission current. When the applied bias was increased to −80 V at ~2 min 14 s (or 2.23 min), again there was an increase in emission current, which dropped suddenly when nanotubes experienced 'burn back'. In our experimental setup, there could be nanotubes in the vicinity that were outside the field-of-view of the TEM CCD

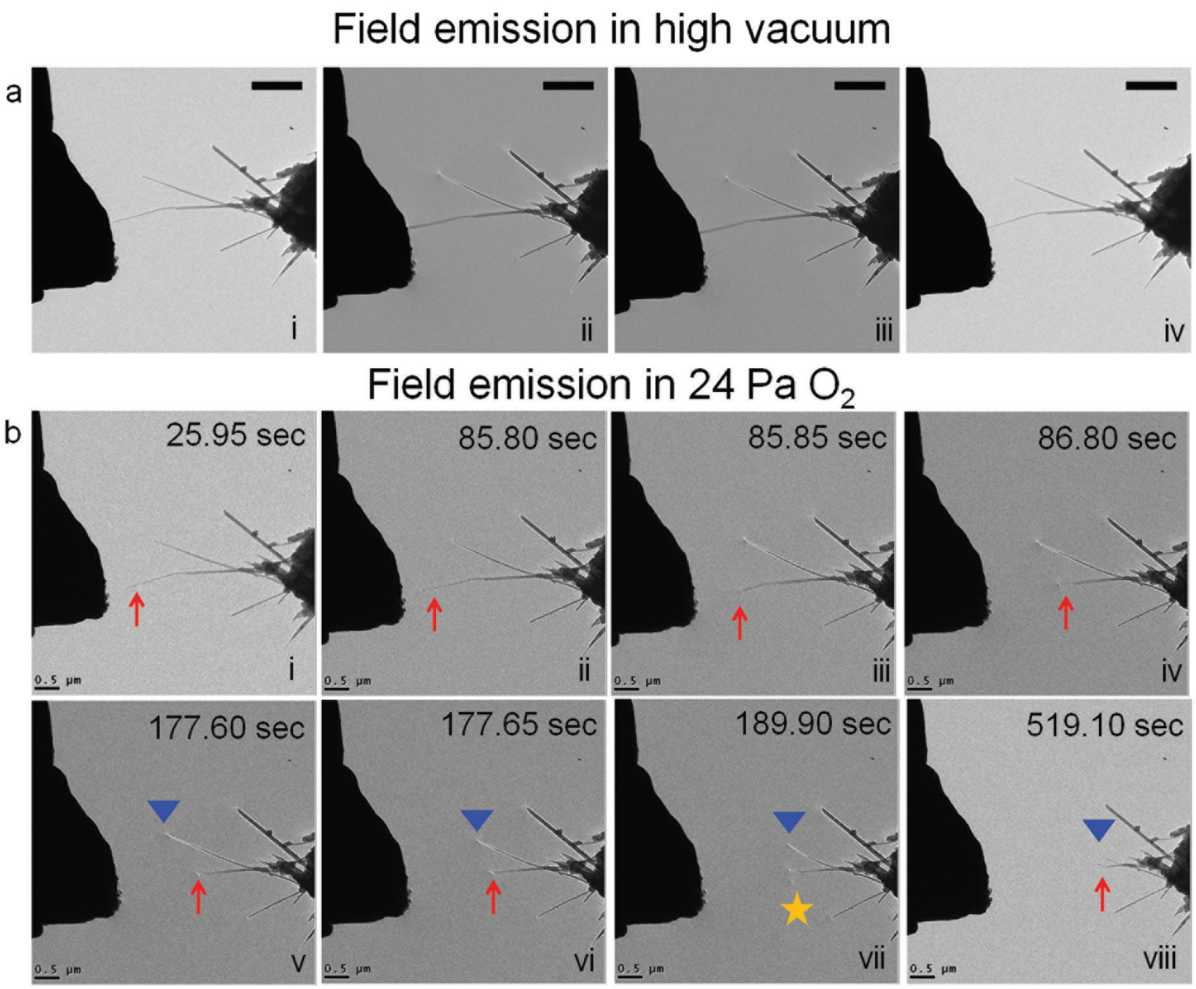

Fig. 2 (a) Field emission behavior from a bundle of carbon nanotubes in high vacuum, (i) at the start with 0 V applied bias, (ii) −80 V applied bias after 1 min; (iii) −80 V applied bias after 10 min and (iv) at the end of the experiment with 0 applied bias. There are no visible changes in the nanotube array. (b) Field emission behavior from the same bundle of carbon nanotubes in 24 Pa of oxygen. CNTs have applied voltages of (i) 0 V, (ii) −50 V, (iii–iv) −70 V, (v–vii) −80 V, and (viii) 0 V. The time stamps of the video clip are indicated at the top of each image. A comparison of the start and end images ((i) and (viii)) show visible reductions in carbon nanotube lengths after being field emitted in oxygen. Scale bar equals 1 μm in panel (a), and 0.5 μm in (b).

camera that were also field-emitting, which would also contribute to the total emission current. Since these nanotubes were at different distances from the probe, and some of which may not be captured by the TEM CCD camera, it was not possible to directly correlate the stability of the field emission current along with the structural changes.

Correlative Lorentz and aberration-corrected, high-resolution TEM imaging

Although the field-free (Lorentz) imaging condition allows us to visualize the field emission process and the influence of the electric field, its spatial resolution (currently about 2 nm at best) is not sufficient to resolve the structural changes in the nanotubes at the atomic level. This is further exacerbated by the distortions caused by the electric fields along the nanotubes, and especially at the tip where the field is most highly concentrated and most structural changes are expected to occur. In order to examine if structural changes have indeed taken place in the nanotubes from high vacuum and oxygen field emission, we performed a series of correlative Lorentz and high-resolution, aberration-corrected TEM imaging (ACTEM) experiments on the *same* carbon nanotubes. The aberration correction is necessary to resolve the graphene layers at 80 kV imaging voltage. By studying the same carbon nanotubes during both high vacuum and oxygen field emission, changes in their structure can be analyzed and compared without any ambiguity.

Fig. 4a(i) shows an ACTEM image of a few nanotubes acquired at the start of the experiment in high vacuum. Fig. 4a (ii–iv) are higher-magnification images of CNTs 1–3 respectively, showing that their tips are closed, and amorphous carbon overcoat surrounds the sidewalls and tips. We then turned off the objective lens of the ETEM and re-aligned the spherical aberration Cs corrector in Lorentz mode (alignments

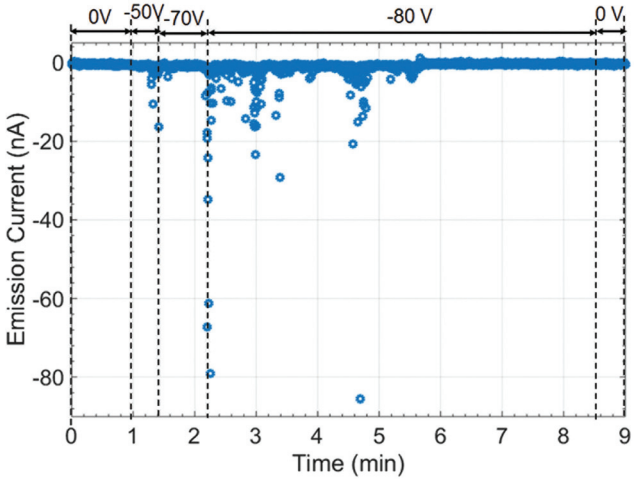

Fig. 3 Corresponding emission current time series plot for *in situ* oxygen field emission data presented in Fig. 2(b). The times at which the applied voltage was increased to −50 V, −70 V and −80 V successively are indicated by the vertical dashed lines (see text for discussion).

were done on the amorphous carbon support film of the half-TEM grid away from the CNTs). Following that, we field emitted the nanotubes in high vacuum (10^{-5} Pa). Fig. 4b(i–iii) show the field-emitting nanotubes at the start of the experiment (0 V), applied bias of −80 V, and at the end of the experiment (0 V), respectively.

After high vacuum field emission, the objective lens was switched back on, and the Cs corrector was aligned in high-resolution mode (on the amorphous carbon support film of the half-TEM grid away from the CNTs). ACTEM images of the same nanotubes acquired after high vacuum field emission (Fig. 4c) reveal that some of the amorphous carbon at the tip of the nanotubes disappeared, but the tube caps remain closed and there is no apparent change in the structure of the graphitic walls of the carbon nanotubes. This is in contrast to the behavior of CNTs forced to field emit at very high fields and currents whereby CNT damage does occur.[6,12,28–32]

The procedures were repeated on the same nanotube group, in the presence of oxygen gas. The objective lens of the

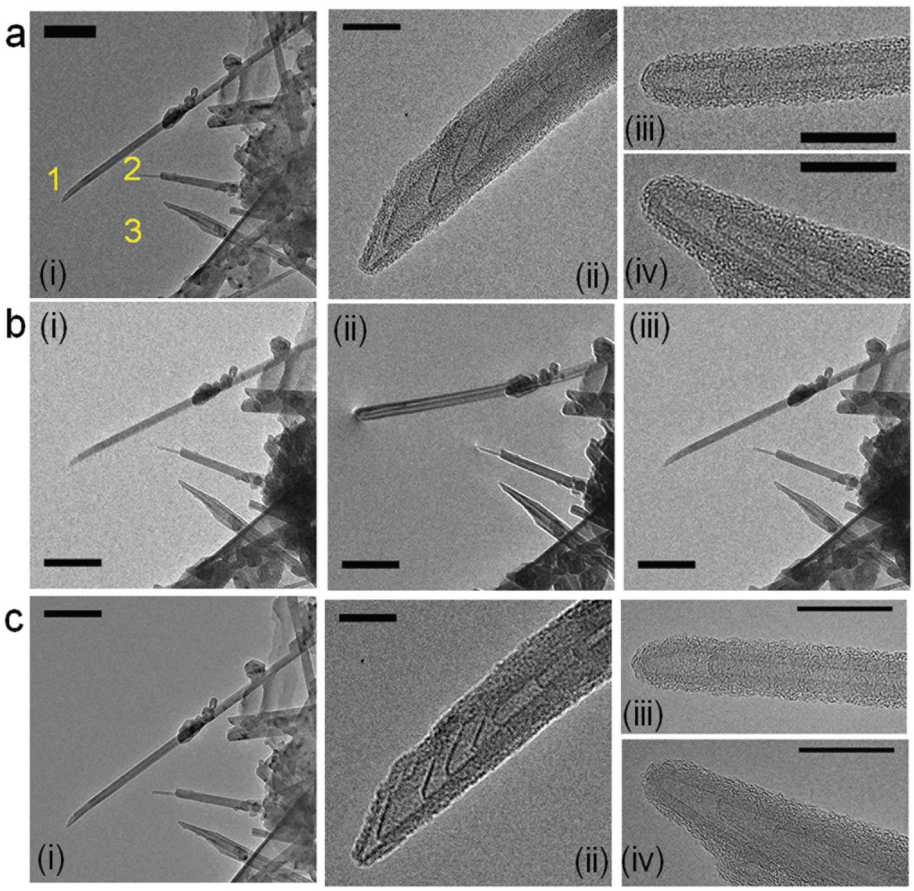

Fig. 4 Structural investigations of carbon nanotubes before, during, and after high vacuum field emission. a(i) shows an aberration-corrected, low magnification pre-degradation TEM image of a few nanotubes at the start of the experiment (before field emission), where a(ii–iv) are higher-magnification images of nanotube 1, 2 and 3 respectively. b(i–iii) show the field-emitting nanotubes at the start of the experiment (0 V), applied bias of −80 V, and at the end of the experiment (0 V), respectively. c(i–iv) are high-resolution images of the same nanotubes after high vacuum field emission. There are no observable differences, even at atomic scale resolution, in the vacuum field emitting nanotubes. Scale bar equals 200 nm in a(i), b(i–iii) and c(i), and 20 nm in a(ii–iv) and c(ii–iv). High-resolution TEM images (panels a and c) have been rotated 90° counterclockwise for correlation to Lorentz TEM images.

ETEM was first turned off. The microscope was re-aligned in Lorentz mode, and 33 Pa of oxygen was introduced. Fig. 5a(i–iv) show the *same* bundle of CNTs presented in Fig. 3, at the start of the oxygen field emission experiment at 0 V, −80 V, −80 V and 0 V respectively. A comparison between Fig. 5a(ii) and (iii) reveals that one of the CNTs had decreased in length by ~110 nm. The electron beam was then blanked and oxygen was purged from the ETEM column. When the base pressure of the microscope returned to high vacuum (10^{-5} Pa), the objective lens of the microscope was switched back on and the Cs corrector was re-aligned in high-resolution TEM mode at high vacuum. Fig. 5b(i–iv) show ACTEM images of the same nanotubes after the oxygen field emission. Clearly, part of Nanotube 1 (b(ii)) broke. A comparison between Fig. 4c (i) and 5b(i) show that Nanotube 1 has decreased by ~115 nm. Furthermore, even though CNTs 2 and 3 did not experience length decreases while field-emitting in oxygen, the ACTEM images revealed that their outermost layers were in fact removed, as indicated by the red arrows in Fig. 4b(iii and iv), and that the nanotube caps are opened.

Fig. 6a(i) depicts another bundle of CNTs in which correlative field emission and high resolution TEM studies were performed. Fig. 6a(ii) is a higher magnification of the inset of Fig. 6a(i) acquired at the start of the experiment. There are four nanotubes (marked A to D) in the bundle, and all had closed caps. The nanotubes were field emitted in high vacuum in Lorentz TEM mode (Fig. 6b). The bright contrast at the nanotube tip which is associated with field emission was observed at applied biases of −70 V (Fig. 6b(ii)) and −90 V (Fig. 6b(iii)). ACTEM images acquired after the high vacuum field emission process show no change in nanotube structures (Fig. 6c). After this observation, the nanotubes were then field emitted in 42 Pa of oxygen in Lorentz TEM mode. Fig. 6d(ii) shows a single emission spot at the tip during oxygen field emission with −70 V bias. When the applied bias increased to −90 V, the number of emission spots increased to two (Fig. 6d(iii)). The applied bias was then reduced to zero and O_2 was purged from the microscope. A comparison between Fig. 6d(i) and (iv) show that the nanotubes had decreased in length. When the ETEM was returned to, and re-aligned in, high resolution mode, we observed that nanotubes A and B experienced length reductions of 85 nm and 88 nm respectively. The side walls of CNT C were destroyed and the outermost caps of C and D were open. Our correlative Lorentz and high resolution studies confirm that the presence of multiple emission spots is due to multiple nanotubes in one bundle. These correlative observations were repeated on more than 20 CNTs. Each round of correlative measurements typically takes 4–5 hours to perform, with 2–4 CNTs being examined.

Previously, Doytcheva and coworkers[31] had studied the degradation of a few CNTs in high vacuum, under high applied currents and voltages, and had observed multiple emission spots which they had attributed to the splitting of the apex of a single nanotube. However, our correlative studies show that the multiple emission spots are in fact due to the breaking up of a bundle of CNTs, presumably through the removal of the amorphous carbon overcoat surrounding the nanotube bundle during the field emission process. Our ACTEM data reveal nanotube shortening and cap and side wall destruction, but we did not observe any nanotube splitting. In that same study,[31] the authors also observed shortening of the nanotubes, and had hypothesized that the application of a

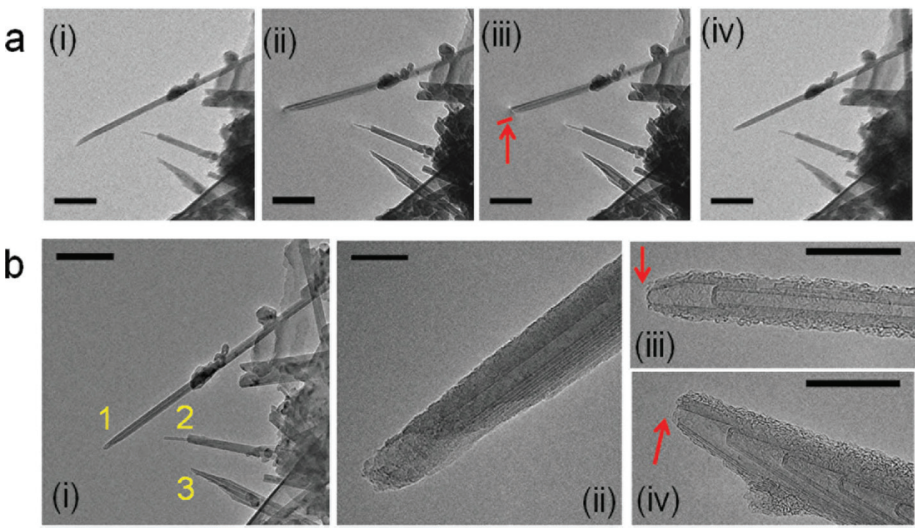

Fig. 5 Structural investigation of the same set of carbon nanotubes in Fig. 3, during and after field emission, in 33 Pa of oxygen. Panel a(i–iv) show the field-emitting nanotubes at the start of the experiment (0 V), applied bias of −80 V, a decrease in length by ~110 nm in one of the nanotubes at −80 V, and at the end of the experiment (0 V), respectively. The solid red line in a(iii) shows the segment of Nanotube 1 which had been removed. b(i–iv) are high-resolution images of the same nanotubes after field emission in oxygen. Opening of tube caps is evident after the field emission step. Scale bar equals 200 nm in a(i–iii) and b(i). Scale bar equals 20 nm in b(ii–iv). Images in panel b have been rotated 90° counterclockwise from the originals for correlation to Lorentz TEM images.

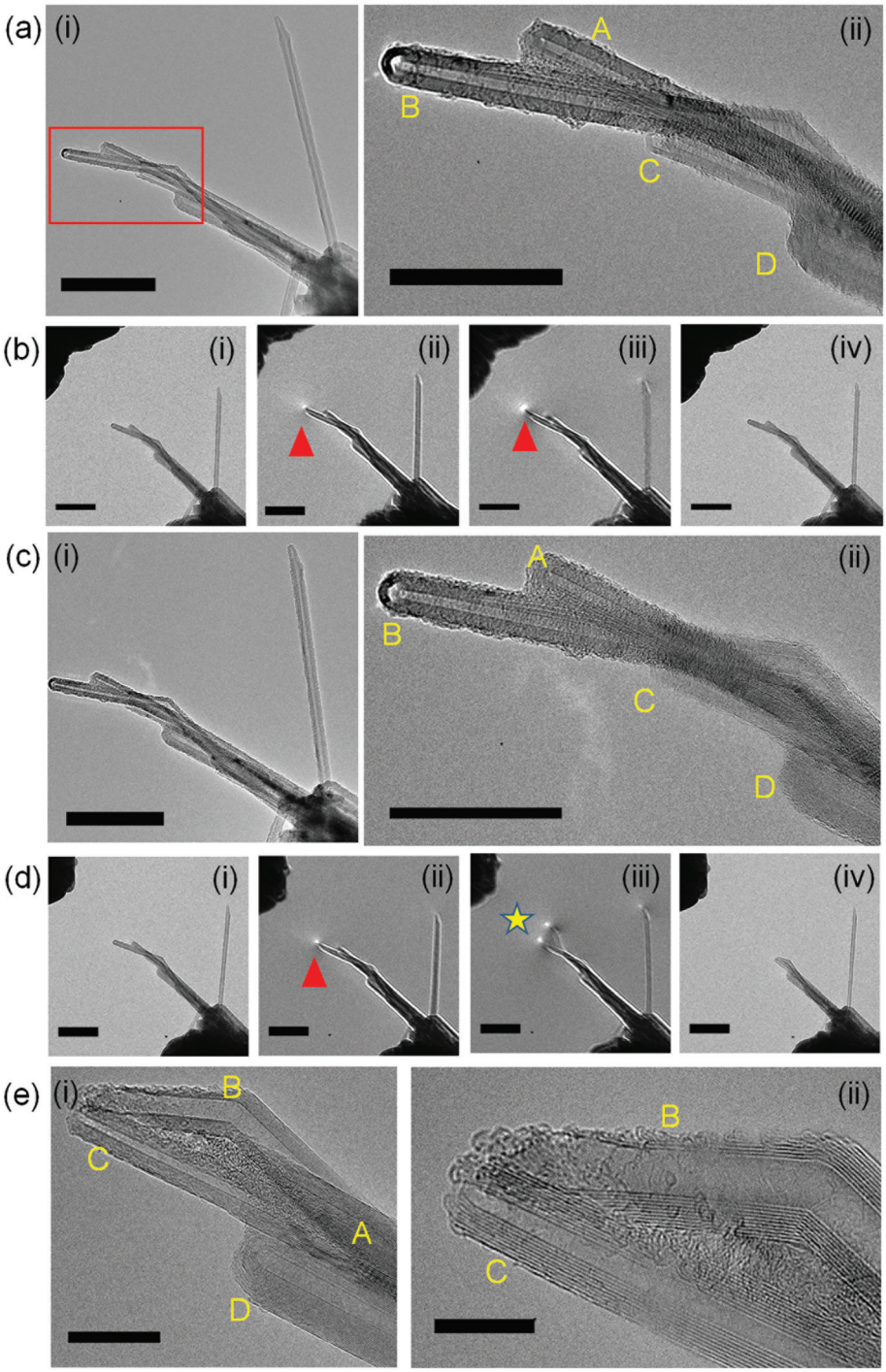

Fig. 6 (a) ACTEM images of a bundle of CNTs at the start of experiment. (b) Field emission in high vacuum (Lorentz mode) at (i) 0 V, (ii) −70 V, (iii) −90 V, (iv) end 0 V. (c) ACTEM images of the same bundle of CNTs after high vacuum field emission, showing no structural changes in the nanotubes. (d) Field emission in 42 Pa oxygen at (i) 0 V, (ii) −70 V, (iii) −90 V, (iv) end 0 V. Multiple emission spots were observed in c(iii) and the nanotubes decreased in length after oxygen field emission. (e) ACTEM images showing structural changes in the same CNT bundle after oxygen field emission. Scale bars equal 100 nm in a(i), (b) and (d), 50 nm in a(ii) and c(ii), 20 nm in e(i) and 10 nm in e(ii).

large electric field leads to charging of the nanotube at a defect point in the outer wall,[28] which breaks a bond in the carbon network at a certain point, which could induce the breaking of a carbon chain in the direction perpendicular to the tube axis and subsequently lead to the whole upper portion of the nanotube being removed. Upon carefully examining many *in situ* recordings, we did not find any clear-cut correlation between nanotube defects and their breakage

behavior. However, as we have reported earlier,[16] the CNTs oxidize from the outer wall and this local thinning might weaken the CNTs sufficiently to promote failure at these locations, which are randomly situated along the CNT.

To test our hypothesis that field emitting nanotubes are likely to ionize the oxygen molecules locally while field emitting in an oxygen environment, we repeated our measurements the same nanotube bundle which was reported in Fig. 6, by performing a second cycle of high vacuum and oxygen field emission. For the sake of clarity, Fig. 6e(ii), which is an ACTEM image of nanotubes B and C after the first oxygen field emission in 42 Pa of oxygen, has been reproduced as Fig. 7a. Fig. 7b and c show the same nanotubes after having been field emitted in high vacuum the second time, followed by the second oxygen field emission in 38 Pa of oxygen. The data suggest that high vacuum field emission removes some of the amorphous carbonaceous material, but the nanotubes appeared to remain largely the same. However, upon the second oxygen field emission, nanotube B experienced further degradation at its side walls (red arrows). Its other side walls were also damaged. These observations confirm our postulation that the voltages and emission currents that were applied in our study do not damage the nanotubes in high vacuum. However, during oxygen field emission, the electric current ionizes the oxygen molecules likely to O_2^+ which are then attracted to the negatively biased CNTs, thereby attacking both caps and side walls of the nanotubes.

Quantification of electron dose

In the gas environment of an ETEM, ionization of gas molecules as a result of the interaction between fast electrons and gas can lead to increased reactivity.[34] To determine, or ameliorate, the influence of the imaging electron beam in our *in situ* field emission experiments, we recorded the corresponding electron dose flux (measured in units of number of electrons per square Ångström per second, e^- Å^{-2} s^{-1}) during the measurements. This parameter had been calibrated for the instrument using a TEM holder with a Faraday cup. The influence of the electron beam was quantified by plotting the cumulative electron dose (expressed in units of number of electrons per square Ångström) *versus* pressure. The typical electron dose flux in Lorentz mode during sample search and focusing, before field emission experiments, was ~0.04 e^- Å^{-2} s^{-1} (4 e^- nm^{-2} s^{-1}), and that during field emission experiments was ~0.25 e^- Å^{-2} s^{-1} (25 e^- nm^{-2} s^{-1}), and so the cumulative electron dose was ~32 e^- Å^{-2} (3200 e^- nm^{-2}) when we first observed abrupt decreases in carbon nanotube lengths during oxygen field emission (which usually occurred 30 s into the field emission experiment, and assuming 10 min of sample search and focusing time). We had previously established a cumulative dose of 1.3×10^4 e^- Å^{-2} (1.3×10^6 e^- nm^{-2}) to cause onset of visible damage to the carbon nanotubes at room temperature arising from gas ionization of up to 100 Pa.[16] Hence we are certain that the electron beam does not influence the field emission experiments in the oxygen environment of the ETEM. For the high vacuum field emission experiments, the cumulative electron dose in the maximum 15 min field emission studies was 250 e^- Å^{-2} (2.5×10^4 e^- nm^{-2}). We had previously established a cumulative dose of 1.2×10^6 e^- Å^{-2} (1.2×10^8 e^- nm^{-2}) to cause onset of visible damage to the carbon nanotubes from continuous electron beam irradiation.[17] Therefore, our high vacuum field emission measurements are not likely to be influenced by the electron beam as well. Data on cumulative electron dose in various conditions are summarized in Fig. 8.

These unique experiments, combined with previous suggestions, provide significant insight into the mechanism of carbon nanotube behavior under field emission conditions. Firstly, CNTs field emitting just beyond their threshold in good vacuum (10^{-5} Pa or better) provide a stable current (ESI Fig. S1†). High-resolution TEM on the *same* nanotubes, before and after field emission, shows that their structure is not altered, beyond the removal of peripheral amorphous adherents. On the other hand, when field emitting in a relatively mild oxygen environment (*ca.* 10^1 Pa here), the average field emission current fluctuates and the CNTs are observed by *in situ* TEM to show a sudden, "episodic" decrease in length (which has been termed "burn-back" by some authors[12]). It is quite clear from the *in situ* recordings that, following these catastrophic events, the CNTs continue to field emit, which is beneficial for the long-lasting field emission properties of a CNT aggregate. Aberration corrected TEM on these CNTs

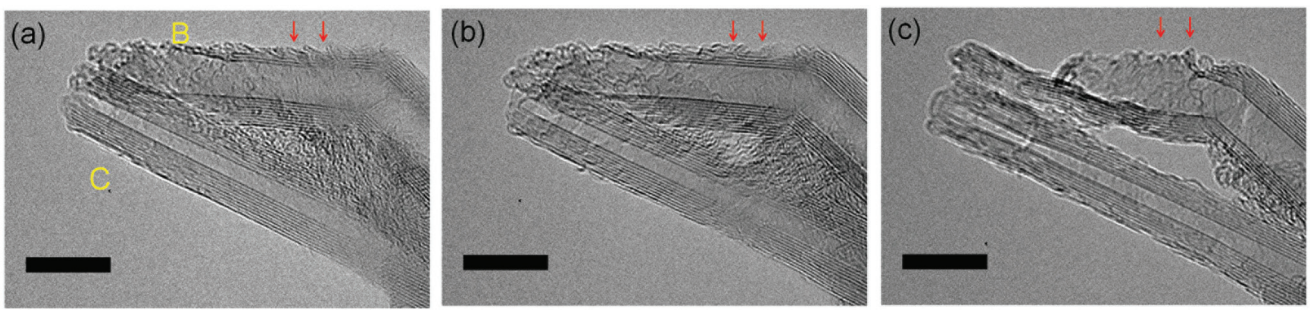

Fig. 7 Aberration-corrected TEM imaging of Nanotubes B and C after (a) first oxygen field emission in 42 Pa O_2, (b) second high vacuum field emission and (c) second oxygen field emission in 38 Pa O_2. No changes are observed between (a) and (b), but there is significant dissipation between (b) and (c). Scale bars equal 10 nm.

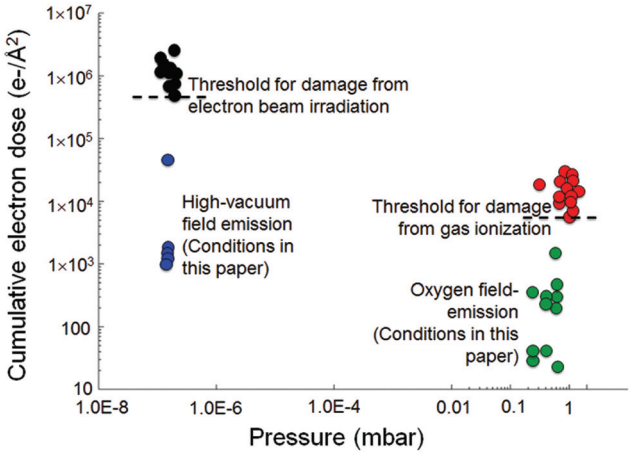

Fig. 8 Cumulative electron dose recorded for field-emission experiments in high-vacuum and oxygen environments. Data points in black and red are from ref. 17. The cumulative electron doses are below the threshold for visible damage in both cases and so the imaging beam does not influence the field emission experiments. 1 mbar equals 100 Pa.

reveals that the nanotube caps are opened both before and after burn-back. Rinzler *et al.* had suggested tube cap opening during field emission in a similar oxygen background pressure ("several mTorr" or 10^{-1} Pa) although they were unable to confirm this proposal by high resolution TEM due to vibrations at the ends of their nanotubes,[12] with burn-back occurring on a much larger scale than ours (10 μm compared to ~100 nm) when the applied bias was increased, observed using an optical microscope connected to a charge-coupled device (CCD) camera.

Other speculations by these authors were not observed in the present study, as well as in earlier high vacuum field emission studies,[31] for instance the unraveling of the CNT plane by plane or the formation of single carbon atom wires from the end of the CNT, which was the main suggestion of that paper.[12] Other studies have suggested field *evaporation* (*i.e.* applying a positive bias to the carbon nanotubes) – as opposed to the application of a negative bias in field emission – to be the more effective way to controllably shape nanotubes,[32,35] and that the excellent field emission characteristics of these CNTs resulted mainly from the irregular shaped graphitic sheet having many dangling bond states around its edges[36] rather than from the linear chains as originally proposed by Rinzler *et al.*,[12] albeit the absence of atomic resolution data clarifying the structural changes at the tube caps. Accordingly, it would be interesting to study the structure of field evaporated CNTs compared with those which have been field emitted, but this is outside the scope of the present paper.

The tube cap openings are consistent with our previous findings on CNTs in an ionizing environment. CNTs exposed to oxygen at elevated temperatures with no imaging beam do not preferentially oxidize at the tube caps, but rather at the side walls.[16,37,38] However, when exposed to the TEM imaging beam at room temperature, some ionization of the oxygen molecules takes place (as verified by electron energy loss spectroscopy) likely creating O_2^+ species. We have proposed that these ions are attracted to the CNTs by image charge forces, thus preferentially oxidizing or etching the CNT caps.[16] In oxygen field emission, oxygen ionization is much more likely to occur as the result of the field emitted electrons because of the relevant energy scales required for ionization (closer to 10 eV). The emitted electron current has sufficient energy to ionize the O_2 species and the applied negative bias will attract these ions along the electric field lines to concentrate them at the nanotube caps. Thus, it is the combination of ionized oxygen and applied bias which leads to the cap openings. Once in this state, the jagged, exposed graphene layers will provide an enhanced electrical field compared to the more smoothly curved, closed nanotubes caps giving rise to higher local field emission current which should be sufficiently high to even sublimate the nanotube at these locations, leading to the burn-back phenomenon. This process will be repeated until the nanotube is consumed, step by step, as seen in the *in situ* TEM recordings.

Conclusion

In summary, this work has utilized *in situ* TEM observations of field emitting carbon nanotubes in a controlled atmosphere oxygen environment of approximately 20–40 Pa. The step-by-step degradation, or burn back, of the CNTs has been directly recorded and it occurs between individual 40 ms frames. High resolution TEM imaging of the same nanotubes shows that the CNT caps were opened during this process due to attack by ionized oxygen species, likely leading to higher field emission currents and sublimation of the tube tips. The combination of *in situ* electrical biasing inside an aberration-corrected, environmental TEM has allowed such observations for the first time.

Conflict of interest

O. Z. has equity ownership and serves on the board of directors of XinRay Systems which develops and manufactures CNT field emission X-ray sources.

Acknowledgements

This work is supported by the National Cancer Institute grants CCNE U54CA-119343 (O. Z.), R01CA134598 (O. Z.), and CCNE-T U54CA151459-02 (R. S.). The authors thank Dr Bo Gao of Xintek for providing the raw CNT materials used in this study, and Professor Yi Cui and Dr Hyun-Wook Lee of the Materials Science and Engineering Department at Stanford University for loan of the electrical biasing TEM holder. Part of this work was performed at the Stanford Nano Shared Facilities.

References

1 S. Iijima, *Nature*, 1991, **354**, 56–58.
2 Z. Liu, G. Yang, Y. Z. Lee, D. Bordelon, J. Lu and O. Zhou, *Appl. Phys. Lett.*, 2006, **89**, 103111.
3 Z. Merali, *Nat. News*, 2009, DOI: 10.1038/news.2009.744.
4 *The Economist, Another look inside*, The Economist Newspaper Limited, Jul 30 2009.
5 X. Qian, A. Tucker, E. Gidcumb, J. Shan, G. Yang, X. Calderon-Colon, S. Sultana, J. Lu, O. Zhou, D. Spronk, F. Sprenger, Y. Zhang, D. Kennedy, T. Farbizio and Z. Jing, *Med. Phys.*, 2012, **39**, 2090–2099.
6 J.-M. Bonard, F. Maier, T. Stöckli, A. Châtelain, W. de Heer, J.-P. Salvetat and L. Forró, *Ultramicroscopy*, 1998, **73**, 7–15.
7 S. T. Purcell, P. Vincent, C. Journet and V. T. Binh, *Phys. Rev. Lett.*, 2002, **88**, 15502.
8 K. A. Dean and B. R. Chalamala, *Appl. Phys. Lett.*, 1999, **75**, 3017–3019.
9 J. Liu, A. G. Rinzler, H. Dai, J. H. Hafner, R. K. Bradley, P. J. Boul, A. Lu, T. Iverson, K. Shelimov, C. B. Huffman, F. Rodriguez-Macias, Y.-S. Shon, T. R. Lee, D. T. Colbert and R. E. Smalley, *Science*, 1998, **290**, 1253–1255.
10 V. Datsyuk, M. Kalyva, K. Papagelis, J. Parthenios, D. Tasis, A. Siokou, I. Kallitsis and C. Galiotis, *Carbon*, 2008, **46**, 833–840.
11 K. Balasubramanian and M. Burghard, *Small*, 2005, **1**, 180–192.
12 A. G. Rinzler, J. H. Hafner, P. Nikolaev, L. Lou, S. J. Kim, D. Tománek, P. Nordlander, D. T. Colbert and R. E. Smalley, *Science*, 1995, **269**, 1550–1553.
13 Y. Zhang, M. X. Liao, S. Z. Deng, J. Chen and N. S. Xu, *Carbon*, 2011, **49**, 3299–3306.
14 S. C. Tsang, P. J. F. Harris and M. L. H. Green, *Nature*, 1993, **362**, 520–522.
15 P. M. Ajayan, T. W. Ebbesen, T. Ichihashi, S. Iijima, K. Tanigaki and H. Hiura, *Nature*, 1993, **362**, 522–525.
16 A. L. Koh, E. Gidcumb, O. Zhou and R. Sinclair, *ACS Nano*, 2013, **7**, 2566–2572.
17 A. L. Koh, E. Gidcumb, O. Zhou and R. Sinclair, *Nano Lett.*, 2016, **16**, 856–863.
18 T. W. Ebbesen and P. M. Ajayan, *Nature*, 1992, **358**, 220–222.
19 K. Svensson, Y. Jompol, H. Olin and E. Olsson, *Rev. Sci. Instrum.*, 2003, **74**, 4945–4947.
20 B. W. Smith and D. E. Luzzi, *J. Appl. Phys.*, 2001, **90**, 3509–3515.
21 T. Fujieda, K. Hidaka, M. Hayashibara, T. Kamino, H. Matsumoto, Y. Ose, H. Abe, T. Shimizu and H. Tokumoto, *Appl. Phys. Lett.*, 2004, **85**, 5739–5741.
22 J. Cumings, A. Zettl, M. R. McCartney and J. C. H. Spence, *Phys. Rev. Lett.*, 2002, **88**, 056804.
23 L. de Knoop, F. Houdellier, C. Gatel, A. Masseboeuf, M. Monthioux and M. Hÿtch, *Micron*, 2014, **63**, 2–8.
24 V. Migunov, A. London, M. Farle and R. E. Dunin-Borkowski, *J. Appl. Phys.*, 2015, **117**, 134301.
25 N. de Jonge, M. Allioux, M. Doytcheva, M. Kaiser, K. B. K. Teo, R. G. Lacerda and W. I. Milne, *Appl. Phys. Lett.*, 2004, **85**, 1607–1609.
26 M. Sveningsson, K. Hansen, K. Svensson, E. Olsson and E. E. B. Campbell, *Phys. Rev. B: Condens. Matter*, 2005, **72**, 085429.
27 K. A. Dean and B. R. Chamala, *Appl. Phys. Lett.*, 2000, **76**, 375–377.
28 Z. L. Wang, R. P. Gao, W. A. de Heer and P. Poncharal, *Appl. Phys. Lett.*, 2002, **80**, 856–858.
29 C. Jin, J. Wang, M. Wang, J. Su and L.-M. Peng, *Carbon*, 2005, **43**, 1026–1031.
30 Y. Saito, K. Seko and J.-I. Kinoshita, *Diamond Relat. Mater.*, 2005, **14**, 1843–1847.
31 M. Doytcheva, M. Kaiser and N. de Jonge, *Nanotechnology*, 2006, **17**, 3226–3233.
32 M. S. Wang, J. Y. Wang and L.-M. Peng, *Appl. Phys. Lett.*, 2006, **88**, 243108.
33 M. Okai, T. Fujieda, K. Hidaka, T. Muneyoshi and T. Yaguchi, *Jpn. J. Appl. Phys.*, 2005, **44**, 2051–2055.
34 J. B. Wagner and M. Beleggia, Gas-Electron Interaction in the ETEM, in *Controlled Atmosphere Transmission Electron Microscopy - Principles and Practice*, ed. T. W. Hansen and J. B. Wagner, Springer International Publishing, 2016, pp. 63–94.
35 M.-S. Wang, Q. Chen and L.-M. Peng, *Adv. Mater.*, 2008, **20**, 724–728.
36 M. S. Wang, L.-M. Peng, J. Y. Wang and Q. Chen, *J. Phys. Chem. B*, 2005, **109**, 110–113.
37 R. Sinclair, P. J. Kempen, R. Chin and A. L. Koh, *Adv. Eng. Mater.*, 2014, **16**, 476–481.
38 B. Liu, H. Jiang, A. V. Krasheninnikov, A. G. Nasibulin, W. Ren, C. Liu, E. I. Kauppinen and H.-M. Cheng, *Small*, 2013, **9**, 1379–1386.